Supporting Information

Thermal and mechanical activation of dynamically stable ionic interaction toward self-healing strengthening elastomers

Yan Peng[a], Yujia Hou[a], Qi Wu[a], Qichao Ran[a], Guangsu Huang[a], and Jinrong Wu [a,*]

[a] State Key Laboratory of Polymer Materials Engineering, College of Polymer Science and Engineering, Sichuan University, Chengdu 610065, China.

*Correspondence and requests for materials should be addressed to: wujinrong@scu.edu.cn

Supporting Information

SI Materials and Methods

Table S1-S2

Figures S1-S15

Experimental Section

Material and methods

Materials: Butyl acrylate (BA, > 99.0%, TCI, stabilized with Hydroquinone monomethylether), acrylic acid (AA, > 99.0%, TCI, stabilized with Hydroquinone monomethylether), 2-(Diisopropylamino)ethyl methacrylate (DPA, 97%, Aldrich, stabilized with Hydroquinone monomethylether), 2-(dimethyl amino)-ethyl methacrylate (DMA, 99%, Adams, stabilized with Hydroquinone monomethylether), 2，2-azobisisobutyronitrile (AIBN, 98%+, Adamas), methyl benzoate (MB, 99% +, Adams), ethyl acetate, n-hexane , petroleum ether and methyl alcohol were purchased from Tansoole.com (China). The reactants were used without further purification except BA, which was filtrated through a basic alumina column to remove the inhibitor.

Synthesis: The elastomers were synthesized by one-pot free-radical copolymerization of BA, AA and DPA. In a typical process, 9.74 g (0.076 mol) of BA, 0.94 g (0.013 mol) of AA, 2.77 g (0.013 mol) of DPA, a bit of AIBN and 1.76 g (0.013 mol) of methyl benzoate (as an internal standard for NMR tests) were firstly dissolved in 20 ml ethyl acetate then poured into a 100 ml there-neck round-bottom flask equipped with a magnetic stirrer and an economical allihn condenser. The mixture was bubbled with argon for at least 20 minutes to remove oxygen then stirred at 70 ^{o}C for 8 h under argon atmosphere to polymerize the monomers. After the polymerization, the product was precipitated in n-hexane or petroleum for at least three times. Finally, the product was dried at 40 ^{o}C in a vacuum oven to constant weight. The molecular weight was measured by gel permeation chromatography (GPC) with dimethylformamide (DMF) as the eluent. The synthetic scheme and results are shown in Scheme S1 and Table S1, respectively.

Film preparation: In a typical process, 4 g of SSE-23 was dissolved in 100 ml methanol, and then the solution was poured into a square Teflon mold. After the solvent was slowly evaporated at room temperature, the sample was put into a vacuum oven at 60 ^{o}C for 72 hours. Take the slow formation of ionic bonds into consideration, all the samples are stored under room temperature for 2 days before characterization.

Measurements and methods

Structure: the molecular structures, ball-stick model is obtained by ChemDraw 18.0 and Chem D raw 3D. and the corresponding steric energy is obtained through MM2 Calculation and quality is fixed to 1.

Fourier transform infrared spectroscopy (FTIR): FTIR spectra were recorded using Thermo Scientific Nicolet iS50 FTIR by an attenuated total reflection mode at room temperature. The on-line tracing of ionic bonds is conducted through the transmission mode. The wavenumber scale was from 4000 cm^{-1} to 650 cm^{-1}. The time for cyclic heating and cooling is 20 minutes to heat and 60 minutes to cool. For the detecting of formation of ionic bond, the monomers are monitored after mixing between two KBr slices and the polymer is detected after fusion under 130 °C for 30 minutes.

Nuclear Magnetic Resonance (NMR): ^1H NMR spectra were measured on an Advance III HD 400 MHz spectrometer (Bruker). $CDCl_3$ (δ (^1H) = 7.27 ppm), CD_3OD (δ (^1H) = 3.11ppm and 4.87 ppm) were used as the solvents.

The molar fractions of BA, AA and DPA in the final products were obtained by calculating the difference of monomer contents before and after the polymerization with MB as the internal standard.

Dynamic mechanical analysis (DMA): Dynamic mechanical was measured on Q800 (TA Instrument) in a tension mode. The rectangle samples with 20 mm in length, 7 mm in width, about 1 mm in thickness were heated and cooled between -40 ^oC to 130 ^oC at a heating and cooling rate of 3 ^oC/min. Dynamic mechanical properties were acquired using a frequency of 1 Hz and a preload force of 0.01 N.

The stress relaxation test is also carried on Q800 (TA Instrument) in a tension mode. The strain is 2% and displace time is 4 minutes. The heat treatment is 60 ^oC for 2 hours and room temperature for 11 hours.

The creep recovery test is also carried on Q800 (TA Instrument) in a tension mode. The stress is 0.01 MPa, displace time is 50 minutes and recovery time is 120 minutes.

Differential scanning calorimeter (DSC): Heat flow curves of SSEs were obtained on Q2000 (TA instrument) with the mass of all samples ranging from 3 mg to 8 mg. The heat flow was recorded from -50 ^{o}C to 100 ^{o}C at a heating rate of 10 ^{o}C/min. The glass transition temperature (Tg) of the sample was defined as the inflection point of the heating curve. The heat treatment is 60 ^{o}C for 2 hour and room temperature for 11 hours.

Rheology: The rheological measurements were performed using an Anton Paar (MCR302). Frequency sweeping from 0.1 to 100 rad/s were conducted with a strain of 0.1 % at room temperature. The sample was a disk with diameter 8 mm and thickness 0.7-1.0 mm and the tests were performed in torsion mode. After 11 hours, the frequency sweeping with the same condition is applied again. The mechanical treatment is carried out at the same machine. Different strain of 20% is applied to the sample within 60 s, then the storage modulus versus time is recorded with strain at 0.1%. The heat treatment is 60 ^{o}C for 2 hours and room temperature for 11 hours.

Atomic force microscopy (AFM) : Sample preparation: In a typical procedure, SSE-23 was dissolved in methanol with a concentration of 0.2 mg/ml. The solution was dip-coated on a silicon slice at room temperature. The silicon slice was then placed in a vacuum oven at 40 ^{o}C for 5 hours to completely dry the sample. The heat treatment is 130 ^{o}C for 20 minutes and room temperature for 4 hours. AFM maps were carried out on an AIST-NT SPM SmartSPMTM-1000 in a tapping (AC) mode with a spring constant of 70 N/m and a resonance frequency of 289.09 kHz.

Small angle X-ray scattering (SAXS): SAXS test is carried out on Xeuss 2.0 (Xenocs) with the wavelength of 0.154 nm and sample-to-detector distance of 2.47 m. The sample is cut into a 5 mm × 5 mm× 0.7 mm slab and the exposure time is 5 minutes. The one-dimensional scattering patterns: Iq^2 as a function of q is obtained by lorentz transformation of the two-dimensional SAXS patterns via a foxtrot software. The heat treatment is 60 ^{o}C for 2 h and room temperature for 11 hours.

Tensile test: Tensile experiments were performed on a tensile tester (SANS CMT 4503). Uniaxial tensile measurements were carried out in the air at room temperature with a strain rate of 0.067 s^{-1}. The dumbbell shaped samples were cut using a normalized cutter. The dumbbell shaped samples have a central part of 25 mm in length, 4.2 mm in width and 0.5-1 mm in thickness. The heat treatment is 60 ^{o}C for 2 h and room temperature for 25 hours. For the cut samples, the treatment is 60 ^{o}C for 5 h and room temperature for 25 hours

Cyclic tensile tests were also performed on the same machine with the strain rate of 0.067 s^{-1}. For each sample, stress-strain curves during the loading and unloading processes to each maximum strain were recorded for five times.

Broadband dielectric relaxation spectrum (BDS): Dielectric measurements were carried out on a Novocontrol Concept 50 system with Alpha impedance analyzer and Quatro Cryosystem temperature control. Frequency sweep from 10^{7} Hz to 10^{-1} Hz was conducted at 100 °C, with temperature stability better than 0.1 K. The disk-shaped film with 0.9 mm thickness and 10 mm in diameter was placed into two parallel copper electrodes.

Theoretical calculation

Toughness: The toughness was calculated by the integrated area below the stress-strain curves as illustrated by the following equation:

$$Toughness = \int_{0}^{\varepsilon_b} \sigma \, d\varepsilon$$

where the σ stands for the stress; ε stands for the strain. ε_b is the fracture strain.

Self-healing efficiency: The self-healing efficiency was calculated by the ratio between fracture stress of cut sample and that of uncut sample, as follows:

$$Healing\ efficiency = \frac{A_{cut}}{A_{uncut}} \times 100\%$$

where the A_{cut} and A_{uncut} stands for the mechanical properties (fracture stress or toughness) of sample after cut and healing, and the uncut samples respectively.

The UCM-Gent model

The UCM model is written as:

$$\sigma_{N,v}(\lambda)=\{\frac{2G_vD_e}{1-2D_e}(1-\exp\left(-\frac{(1-2D_e)}{D_e}(\lambda-1)\right)) + \frac{G_vD_e}{1+D_e}(1-\exp\left(-\frac{(1+D_e)}{D_e}(\lambda-1)\right))\}\lambda^{-1} \quad (1)$$

While the Gent strain hardening model is written as:

$$\sigma_{N,e}(\lambda)=\left(\frac{G_e}{1-\frac{\lambda^2+2\lambda^{-1}-3}{J_m}}(\lambda^2-\lambda^{-1})\right)\lambda^{-1} \quad (2)$$

And the combined model is the sum of the above models written as:

$$\sigma_N(\lambda)=\sigma_{N,v}(\lambda)+\sigma_{N,e}(\lambda) \quad (3)$$

Where the λ is the extension ratio, equal to ε+1; and the Gv, Ge is the initial shear modulus for the viscoelastic part (representing the contribution of weak interaction) and small-strain shear modulus for the elastic part (representing the contribution of strong interaction) separately; De is the Deborah number (related to the relaxation time of the viscous component and the strain rate); Jm is the maximum allowable value of the first strain invariant. Since the Young's modulus E = 3(Ge + Gv) which can be obtained from the stress strain curve directly, the combined model Eqn (3) which is determined by four parameters Gv, De, Ge and Jm can be used to simulate the stress strain curve with three independent parameters.

Arrhenius equation

The relax time obtained by stress relax measurement follows Arrhenius' law.

$$\tau = \tau_0 * exp(\frac{E_a}{RT})$$

where E_a is the activation energy, τ is relax time, and τ_0 is a proportionality constant; T is temperature; R is molar gas constant.

Broadband dielectric relaxation spectrum (BDS):

Because of the high content of ionic cluster which leads electrode polarization (EP) and DC conductivity at low frequency, the relaxation of ionic cluster is covered in the frequency-

dependent ε″. To solve this problem, an approach of derivative of the permittivity is used[1]

$$\varepsilon_{der}=-\pi/2(\partial\varepsilon'(\omega))/(\partial(\mathrm{Ln}\omega))$$

Where ε'(ω) is the dielectric constant and ω is the angular frequency.

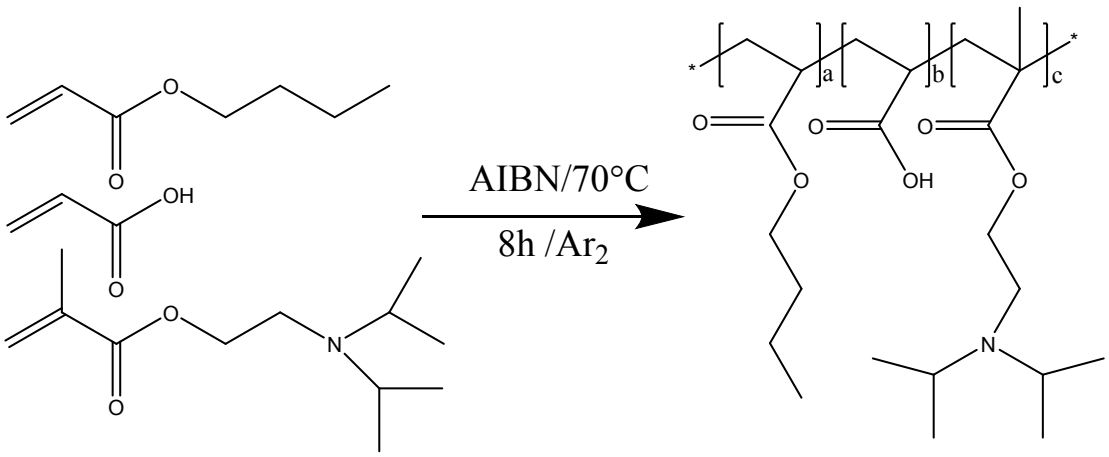

Scheme 1. The synthesis of SSEs.

Table S1. The formula for samples.

Sample	Content of ionic monomers in SSEs ($\frac{n_{anion}+n_{cation}}{n_{total}}$)	Mn (g/mol)	PDI	*Tg*
SSE-15	14.6/100	10827	2.21	-9.9
SSE-23	22.5/100	9341	2.42	-6.02
SSE-35	35.0/100	15432	3.46	9.53
SSE-42	42.2/100	10740	1.6	/
Control sample	22.8/100	45950	2.52	/
BA-AA-DPA-2	23.4/100	/	/	/

Pure PBA	0%	/	/	/

Table S2. The comparation of the existing self-healing material showing healing efficiency higher than 100%.

Material	Self-healing efficiency	Measure method	Healing agent	Healing type	Stable or not at room temperature	ref
Epoxy resin[2]	134%	Mechanical property tests	Pre-embedded healing agent	Only crack	Stable	ref 1
Coating[3]	110%	Electrochemical measurements	Additional Ca^{2+}	Only crack	Stable	ref 2
Elastomer[4]	125%	Mechanical property tests	No	Cut samples and cracks	Unstable	ref 3
Our work	143%	Mechanical property tests	No	Cut samples and cracks	Stable	

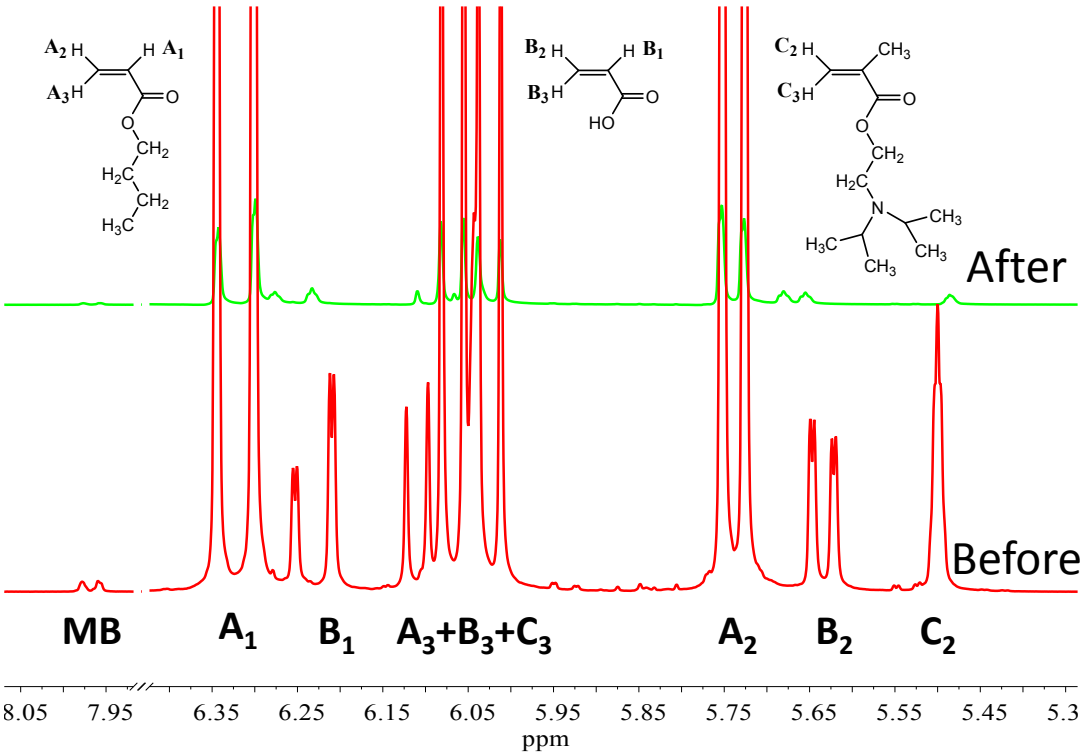

Figure S1. ^{1}H NMR spectra of monomers before (red line) and after (green line) copolymerization. MB is an internal standard.

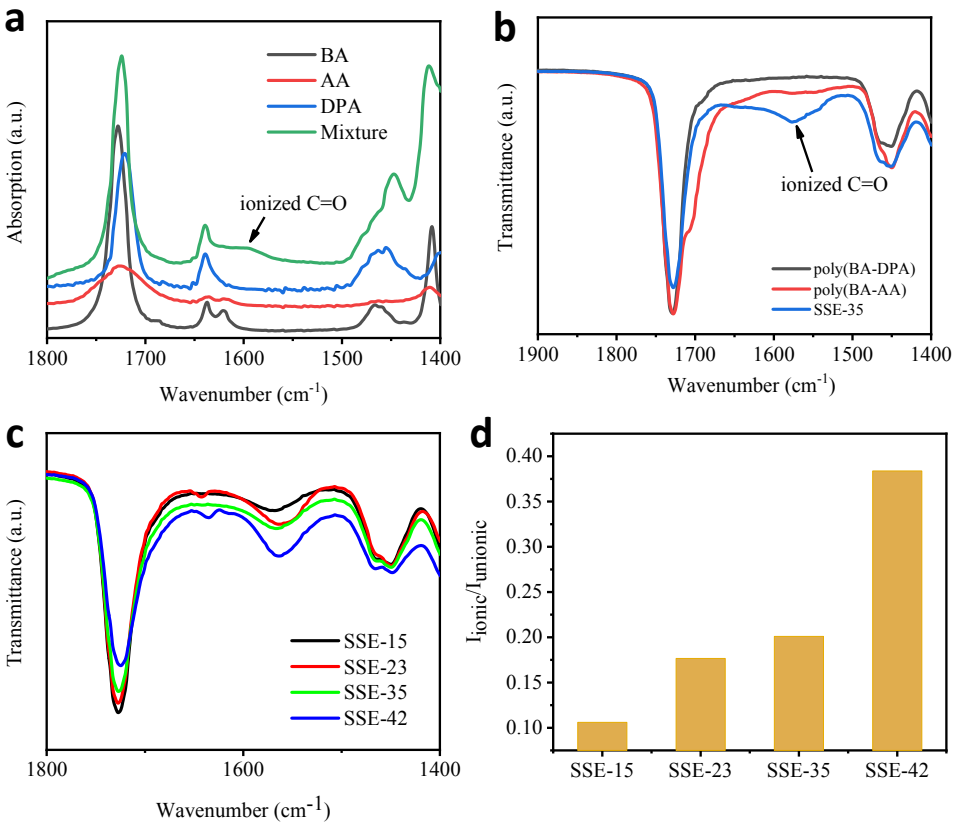

Figure S2. FTIR spectra. a) the FTIR spectra of monomer of BA, AA, DPA and the mixture of BA, AA, DPA. A new peak appear in mixture, which is the stretching vibration ionic C=O. b) the FTIR spectra of poly(BA-AA), poly(BA-DPA) and SSE-35. A new peak appears in SSE, which is the stretching vibration ionic C=O. c), d) the FTIR spectra of SSEs and the corresponding ratio of intensity of ionic C=O to that of Free C=O. The new peak of mixture. These data show that ionic bond is formed due to the AA and DMA. And the intensity of ionic bonds increases with the content of AA and DPA.

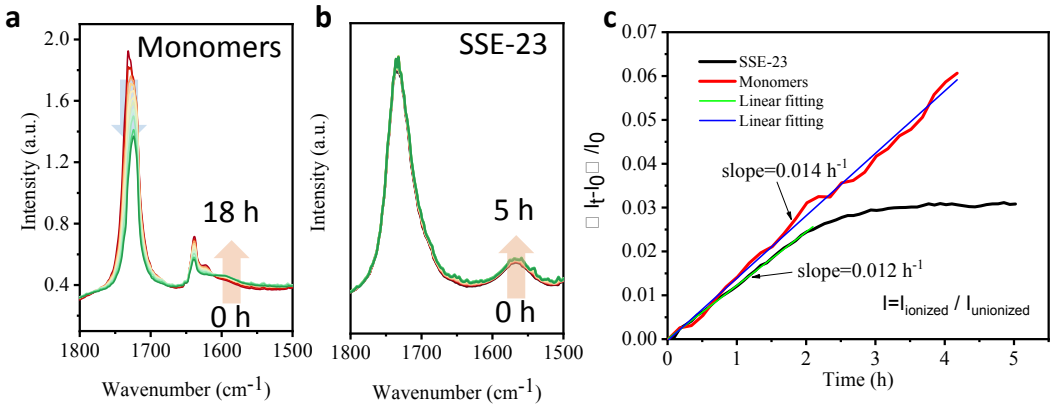

Figure S3. Time-dependent formation of ionic bonds between AA and DPA of monomers and polymer. On-line FTIR absorbance spectra of the monomer mixture of BA, AA and DPA after mixing (a) and SSE-23(b). The ionic peak is 1594 cm^{-1} for monomers and 1570 cm^{-1} for polymer. c) the variation percentage, $(I_t-I_0)/I_0$, as a function of time of the SSE-23 and monomers. The slopes of monomers and SSE-23 are 0.0118 and 0.0142 respectively.

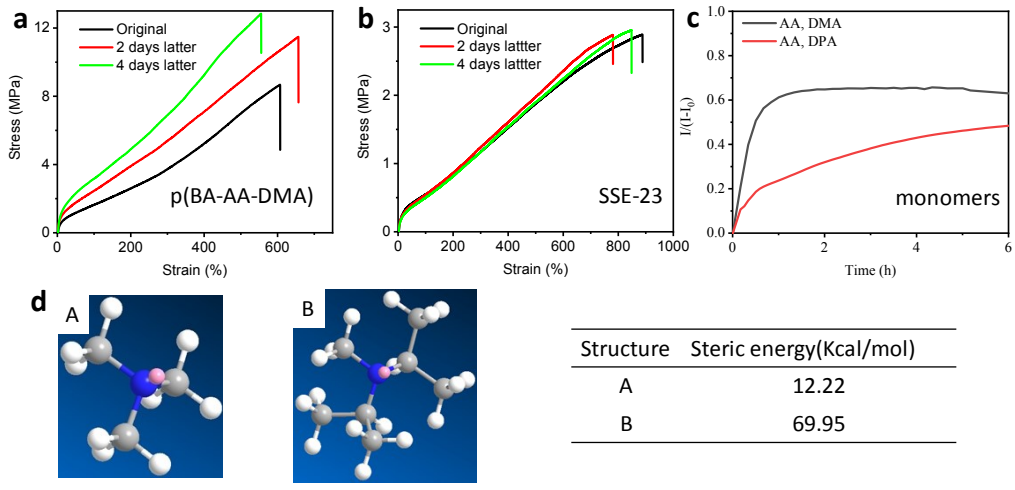

Structure	Steric energy(Kcal/mol)
A	12.22
B	69.95

Figure S4. Stress- strain curves of the p(BA-AA-DMA) (a) and SSE-23 (b) stored at room temperature for different times. c) the formation of ionic bonds between AA and DMA, AA and DPA, which indictes that the AA and DMA can form more ionic bonds and faster. d) the ball and stick model of methylated (A) and isopropylated (B) tertiary and the corresponding steric energy.

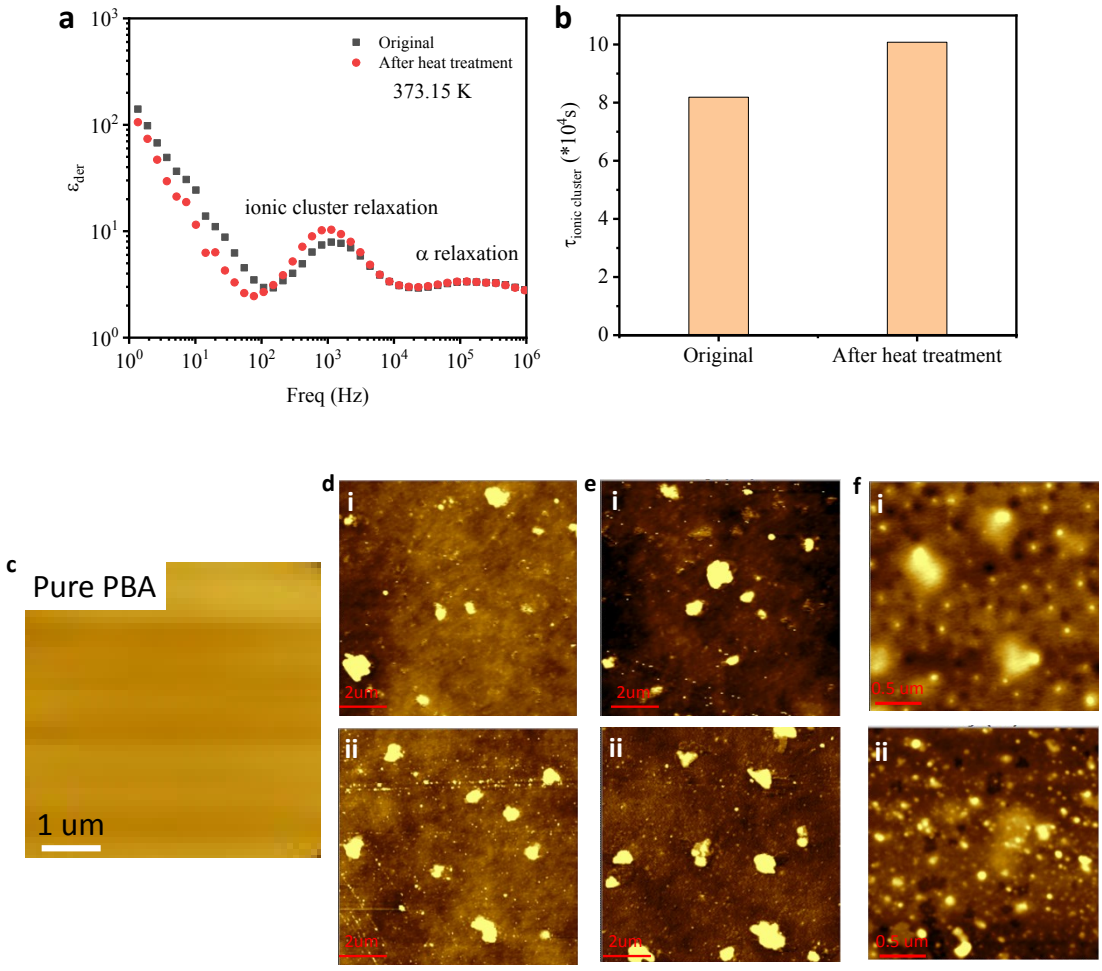

Figure S5. a) The frequency-dependent ε_{der} and b) the relaxation time of ionic cluster (the reciprocal of the frequency at the peak) of SSE-23 at 373.15 K before and after heat treatment (60 °C for 2 h and 25 °C for 25 h). c) AFM phase image of Pure PBA. d), e) AFM phase images before (i) and after (ii) heat treatment of SSE-15 at different places. f) AFM height images before (i) and after (ii) heat treatment of SSE-15.

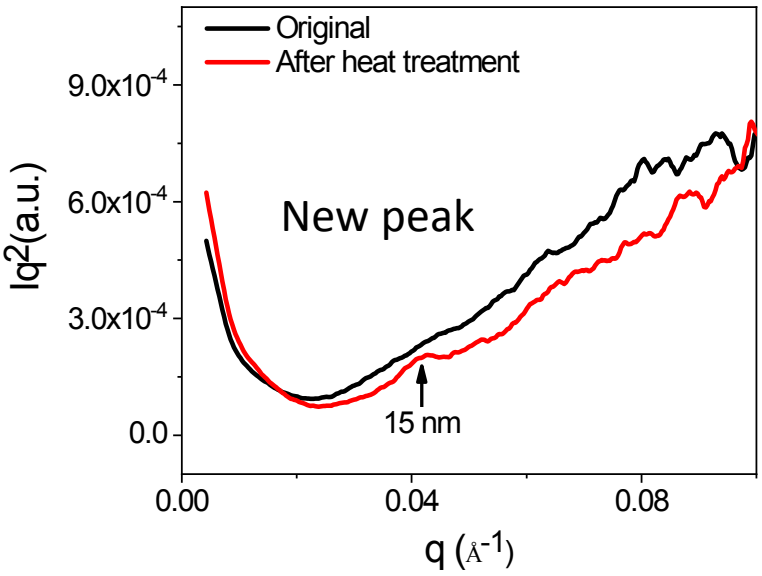

Figure S6. The Iq2 (after Lorentz transformation) versus q from the SAXS tests (SSE-15).

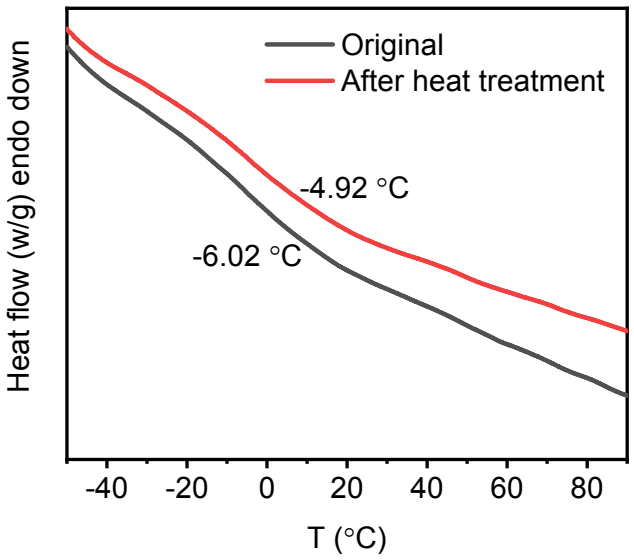

Figure S7. The DSC curves of SSE-23 before and after heat treatment.

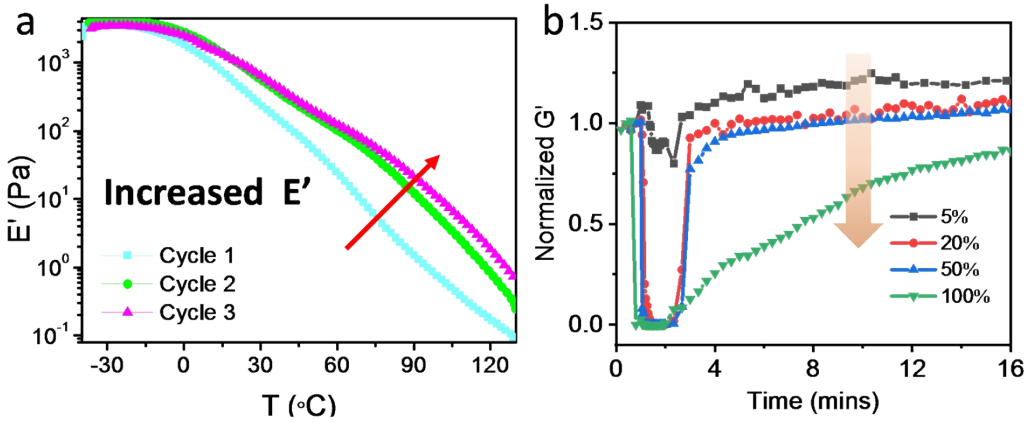

Figure S8. (a) The storage modulus of the cyclic temperature sweeping in DMA test (SSE-42). (b) The normalized storage modulus versus time at room temperature after different shear strain treatment.

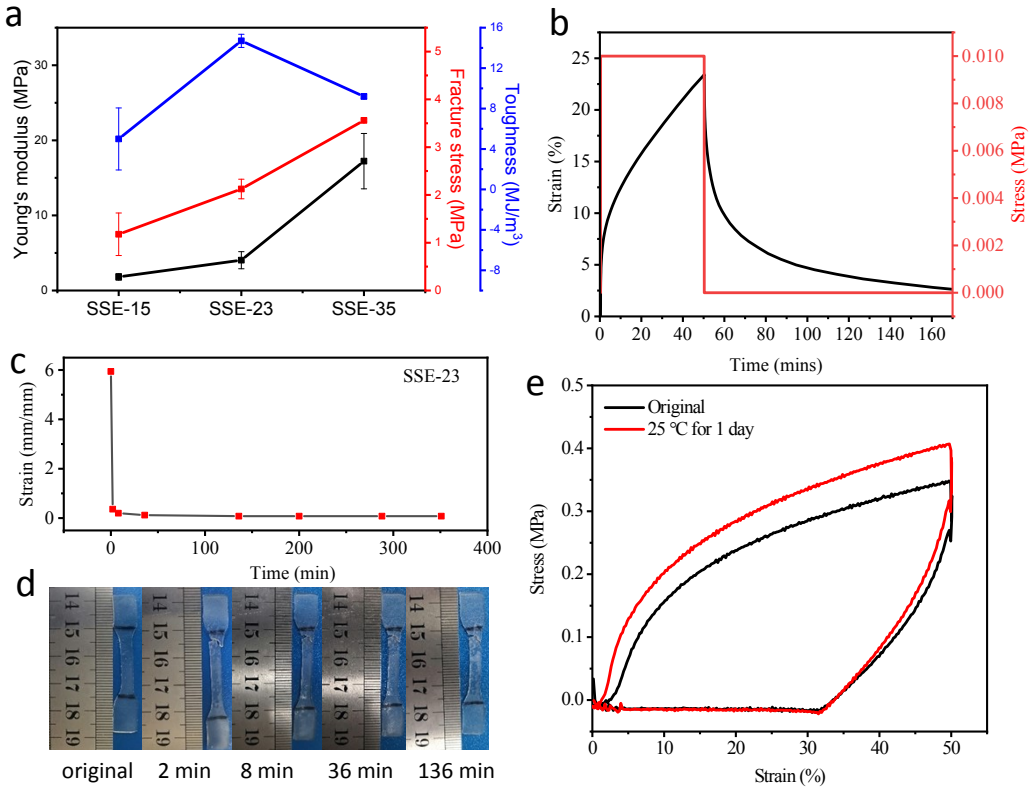

Figure S9. a) The Young's modulus, toughness and fracture stress of SSEs. b) The creep recovery of SSE-15. c) The relative length change versus time of SSE-23 after fracture. L0 is original length of sample, L is the length after fracture. d) Photographs of recovery process of HiSHE-23 after the fracture, which shows that the sample can recover to its original length after 60 min from its fracture length. e) The loading and unloading behavior of SSE-23, the big

hysteresis is due to the energy dissipation of weak ionic bonds. After mechanical destroy and 1 day to heal, the hysteresis loop is bigger, which also indicate a higher energy dissipation.

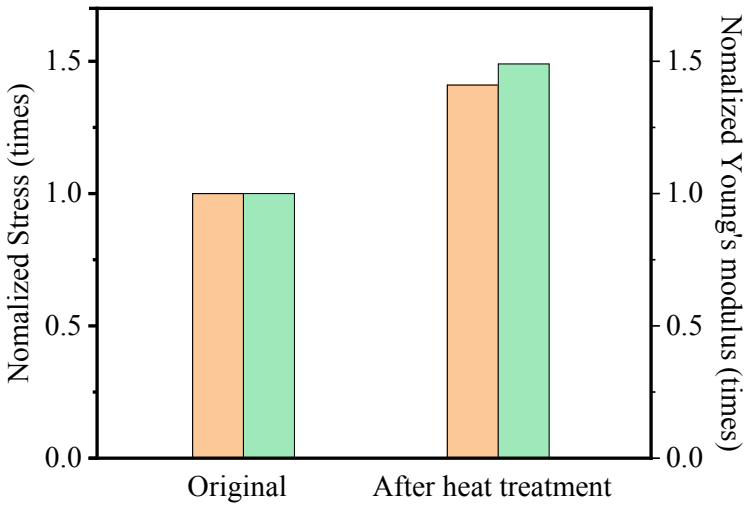

Figure S10. The normalized stress and Young's modulus of SSE-23 before and after heat treatment. The value is calculated from the ratio of average value after heat treatment to the average value of original. Therefore, there is no error bar.

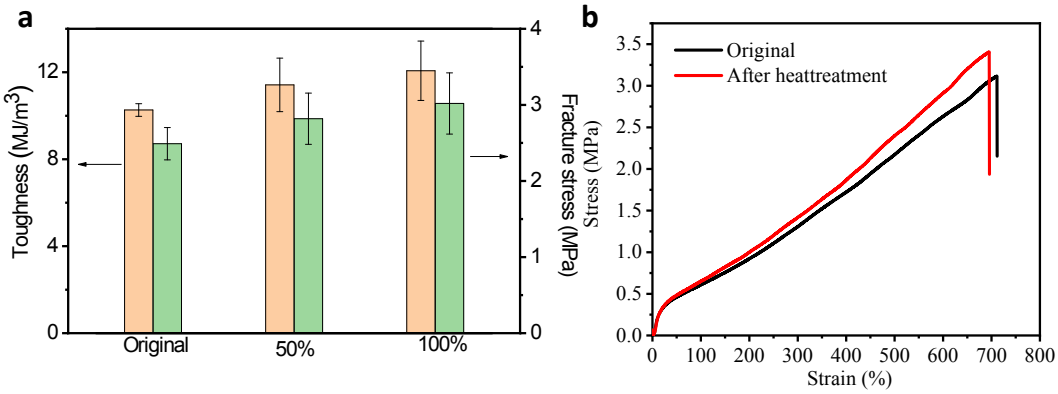

Figure S11. The toughness and stress of SSE-23 before and after different strain treatment. b) the stress strain curves of reproductive (dissolved by solvent and remolded) SSE-23 before and after heat treatment.

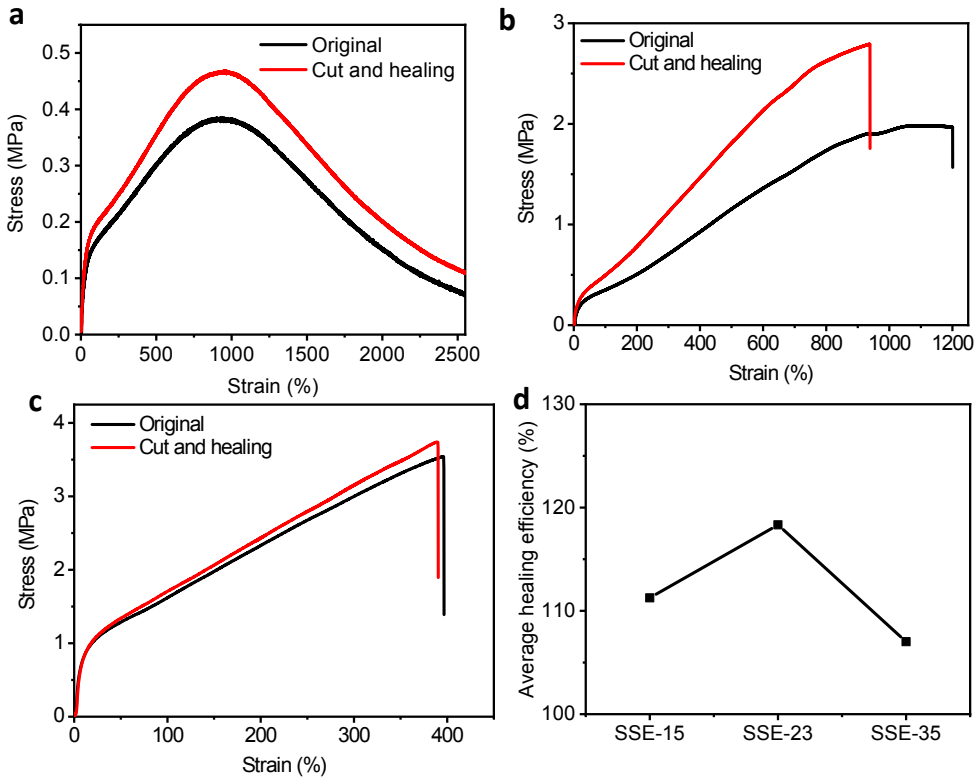

Figure S12. The stress-strain curves of (a) SSE-15, (b) SSE-23, (c) SSE-35 (d) and the corresponding healing efficiency before and after cut and healing (60 °C for 5 hours and RT for 25 hours).

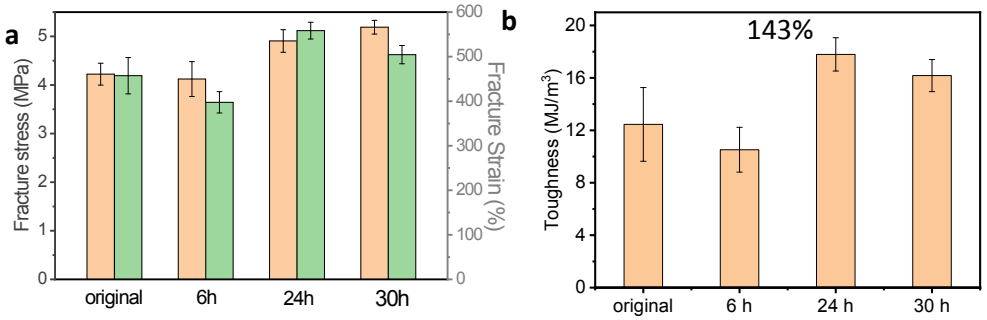

Figure S13. The stress and strain (a) and toughness (b) of SSE-35 after cut and healing for different times.

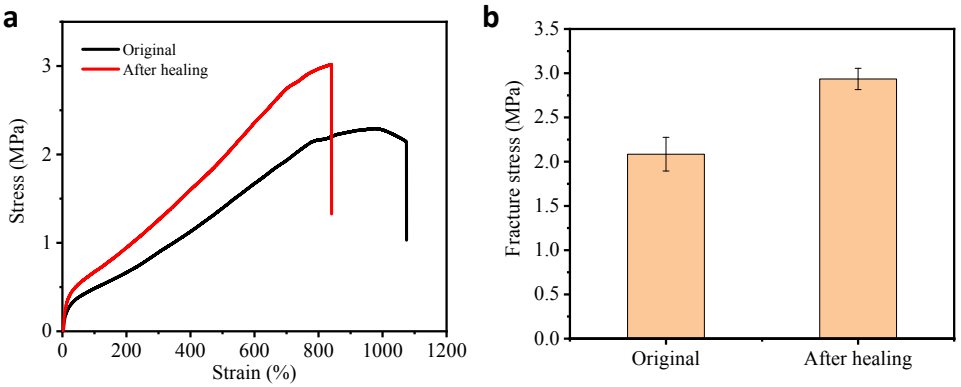

Figure S14. a) stress-strain curves and b) fracture stress of BA-AA-DPA-2 before and after cut and healing (60 °C for 2 hours and 25 °C for 11 hours).

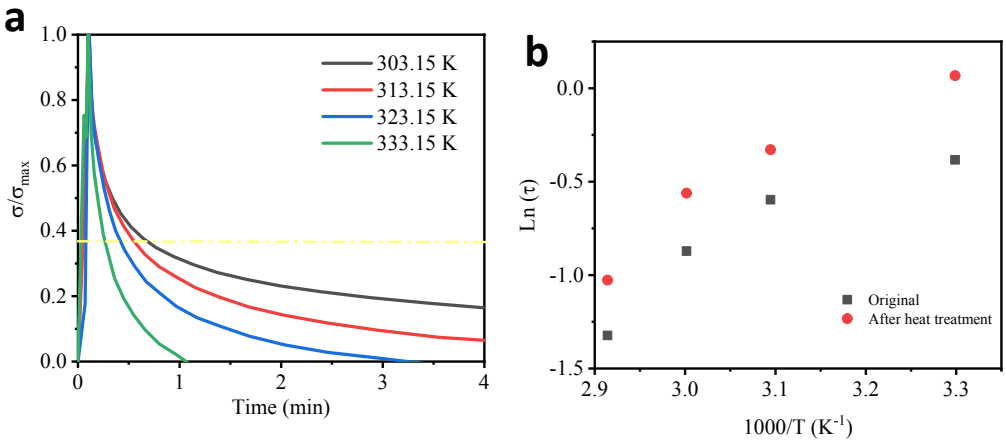

Figure S15. (a) the stress relaxation curves of SSE-23. (b) Arrhenius plot of the measured relaxation time before after heat treatment (60 °C for 2 hours and room temperature for 11 hours.

Reference

1 U.H. Choi, Y. Ye, D. Salas De La Cruz, W. Liu, K.I. Winey, Y.A. Elabd, J. Runt, R.H. Colby. *Macromolecules*, 2014, **47**, 777.

2 G. Romero-Sabat, E. Gago-Benedí, J.J. Roa Rovira, D. González-Gálvez, A. Mateo, S. Medel, A. Tolentino Chivite. *Compos Part A: Appl Sci Manufac*, 2021, **145**, 106335.

3 Y. Duan, Y. Wu, R. Yan, M. Lin, S. Sun, H. Ma. *Prog. Org. Coat.*, 2021, **155**, 106232.

4 Y. Peng, L. Zhao, C. Yang, Y. Yang, C. Song, Q. Wu, G. Huang, J. Wu. *J Mater Chem A*, 2018, **6**, 19066.